LASER-INDUCED FLUORESCENCE MEASUREMENTS TO TEST CHEMICAL MECHANISMS OF PROMPT NO IN METHANE FLAMES

Dwayne E. Heard, Jay B. Jeffries, Gregory P. Smith and David R. Crosley
Molecular Physics Laboratory
SRI International
Menlo Park, CA 94025

ABSTRACT

Laser-induced fluorescence measurements have been made of the OH, CH and NO radicals in slightly rich methane/air flames burning at 30, 70 and 120 Torr; in the 30 Torr flame atomic hydrogen is also measured. Absolute NO and OH concentrations were determined using separate calibration experiments. Temperature profiles were deduced from OH rotational excitation scans, and fluorescence quenching rates for NO and CH were determined. Predicted profiles of the concentrations of these radical species as a function of height above the burner were obtained from a computer model of the flame, and comparison made with experiment. Good agreement is achieved for the relative concentration profiles, the absolute NO concentration, and concentration ratios between 30 and 70 Torr, although slight disagreement with the CH profile indicates there remain some unknown aspects of the flame chemistry.

INTRODUCTION

Although natural gas is a clean burning fuel, containing virtually no fuel-bound nitrogen or sulfur, its combustion in air forms NO_x pollutants. These emissions limit its use, and the degree of regulation is expected to become more stringent in the future. Thus reduction of NO_x emissions in practical natural gas systems is an important objective. A major part of attaining that goal is the development of a predictive computer model of the pertinent chemistry, validated by sensitive laboratory experiments.

At temperatures below 2000 K, the major method of NO production in hydrocarbon/air flames is by the prompt-NO route, especially for slightly fuel-rich conditions. This dominates in practical natural gas/air flames, which usually operate at temperatures below 2000 K. Even though average fuel/oxygen ratios may be on the lean side, there are always locally fuel-rich regions in a nonpremixed flame, which includes most practical burners.

The prompt NO mechanism, whose reactions occur near the flame zone, is largely that first postulated by Fenimore[1] in 1971. Much of this reaction mechanism has recently been extensively reviewed and discussed by Miller and Bowman.[2] The primary initiation reaction is that of the radical CH with the air nitrogen to produce HCN and nitrogen atoms. The HCN undergoes several oxidation steps to produce more N atoms; these atoms then react with OH and O_2 to form NO. Some of the NO can be back-converted to HCN through a series of reactions also involving CH radicals.

Much but not all of this chemistry is well understood. Because the desired level of prompt NO produced in natural/gas air flames is often tens of parts per millions, the reactive species responsible are also present at low concentrations. Accordingly, any sensitive test of the model predictions must involve measurements of these pertinent radical species with a high degree of spatial resolution. We have made laser-induced fluorescence measurements of atomic hydrogen and the free radicals CH, OH and NO in low pressure methane/air flames. The flame studied most extensively was burned at 30 Torr. A computer model of the flame chemistry was used to predict species profiles, and comparisons with experiment were made to identify key aspects of the prompt NO chemical mechanism.

EXPERIMENTAL DETAILS

The flames were supported on a 6 cm diameter porous plug McKenna burner, inside an evacuable chamber suitable for optical probing, described in more detail in Refs. 3 & 4. A shroud of Ar was employed to match the flame velocity at the burner surface and improve flame stability. The flame most extensively studied was slightly rich, with an equivalence ratio of 1.13, and at a pressure of 30 Torr. The high pressure flames were operated at the same equivalence ratio and same total flow rates, so they are positioned much closer to the burner surface. The flow rate was kept constant at all times for all flames studied in this work. All measurements were made using laser-induced fluorescence (LIF); the optical configuration remained the same whilst the burner was translated vertically with a minimum step size of 6 μm. Profiles as a function of height above the surface were typically measured with 125 μm between points and a spatial resolution between 0.2 mm and 1.0 mm.

Following laser excitation the fluorescence was collected at right angles and imaged onto a monochromator with attached photomultiplier (PMT), except in the case of H atoms, for which an interference filter centered at 656 nm was employed. The PMT signal was captured by a boxcar (SRS 250) and stored on computer through a CAMAC crate. Fluorescence lifetimes were measured using a Transiac 2001S 100 MHz digitizer. The laser energy was recorded in order to normalize the LIF signal on a shot-to-shot basis.

Collisions with the ambient flame gases quench the electronically excited states of the radicals, decreasing the fluorescence decay time from that given by the purely radiative rate. In the case of OH, the influence of quenching on the fluorescence quantum yield is avoided by the use of a short (20 ns duration) gate triggered promptly after the exciting laser pulse.[5] For NO and CH, the lower signal levels require integration over a large fraction of the decay pulse, and quenching must be accounted for to determine relative concentration profiles. In the case of NO, the decay time in the flame is also needed to calibrate the absolute concentration by comparison with LIF from a known room temperature concentration.

Decay measurements were made in the 30 and 70 Torr flames for both NO and CH, using the transient digitizer, with 10 ns resolution. The details are reported elsewhere,[6] where the experimental results for the 30 Torr flame are compared to those expected from current knowledge of species—specific cross sections for quenching of $A^2\Sigma^+$ NO and $A^2\Delta$ CH, together with a calculated composition of the flame. The agreement is good, within 20 to 30%. For both CH and NO, total quenching rate and thus fluorescence quantum yield were found[6] to be independent of flame position within experimental errors of 10%.

TEMPERATURE MEASUREMENTS

Accurate temperature determinations are crucial to any meaningful comparison between measured and calculated species profiles. This is because of the highly nonlinear dependence of reaction rates on temperature; it is especially true in the case of prompt NO formation, owing to the considerable temperature dependence for reactions including $CH + N_2$. As discussed below, a systematic error of 40 K through the flame (about 2.5%, and the same as our random error bars) would alter the predicted NO concentration by nearly 25%.

The temperature profiles are also needed to reduce measured LIF intensities to ground state radical concentrations, accounting for the variation of the fraction of the molecules populating the absorbing level as a function of temperature. Accuracy is especially important for this purpose at the lower temperatures close to the burner surface.

LIF temperature measurements are made using rotational excitation scans in the (0,0) band of the OH radical, which provides strong signals throughout the flame. The special care that must be taken to avoid systematic errors in these measurements has been discussed.[7] These include: (1) use of a prompt detection gate, here 20 ns, to avoid problems caused by temperature and

rotational-level dependent quenching and radiative rates; (2) use of a detector with a uniform response over a wide bandpass, here 25 nm, to avoid biasing due to changes in the fluorescence spectrum with excited rotational level; (3) normalizing LIF signals by transmitted laser intensity to correct for non-zero optical depth; and (4) operating in a linear regime to avoid intensity anomalies due to satellites and line wings.

Temperatures were measured in the flame using a spectral fitting method. Fig. 1 shows how spectra taken at different heights above the burner surface vary with temperature. The top panel is near the peak, with a fitted temperature of 1672 K. The middle panel shows a spectrum at 1153 K, while the bottom panel exhibits the sparse spectrum found in the coolest region we could measure, 405 K at only 2.5 mm from the burner surface. Due to the near ambient temperature (achieved through water cooling) heterogeneous reactions at the burner surface are minimized.

The temperature profile in the 30 Torr flames is shown in the top left panel of Fig. 2. Temperature profiles were also measured in the 70 and 120 Torr flames, exhibiting a peak closer to the burner surface, but with approximately the same peak value. The error bars were larger in the higher pressure flames, and have been estimated at about 100 K. A smooth temperature profile was fitted to the data for each flame, and then used as input to the model as well as for analysis of the LIF intensity profiles to obtain species concentrations.

EXPERIMENTAL SPECIES PROFILES

OH--Most profiles were made using the $R_2(6)$ line of the (0,0) band of the A-X system; some checks using the $R_1(3)$ line showed excellent agreement after accounting for the difference in population fraction with temperature. The 20 ns duration, prompt gate avoided effects of quenching.[5] The absolute OH concentration was measured at its peak value by an absorption measurement of 2% per cm for the $R_2(6)$ line and 1.5% per cm for $R_1(3)$, corresponding to a peak concentration of $(6\pm3) \times 10^{14}$ molecules/cm^3, or a mole fraction of 0.0035 in the 30 Torr flame. Similar measurements at 70 Torr indicate approximately the same fractional peak concentration.

NO--The $Q_1(17)$ rotational line of the (0,0) band of the A-X system was used for the profiles, (again minimizing the temperature dependence of the absorption) while collecting the (0,2) fluorescence. The absolute NO concentration was obtained by calibration using LIF in known amounts of NO diluted in helium/argon mixtures, flowing through the burner at room temperature. The optical system was the same as in the flame; the ratio of the LIF signals under these conditions to those in the flame then furnished the desired calibration. In the room temperature flow, the decay is mainly radiative with a lifetime of 192 ns. The quenching rate in the 30 Torr flame at the peak of the NO signal is 2.9×10^7 s^{-1}. Taking the ratio of the two signals and the quenching and accounting for Boltzmann population difference of the absorbing rotational level yielded a peak NO concentration of $(7\pm4) \times 10^{11}$ molecules/cm^3, or a fractional concentration of 4 ppm in the flame. From comparison of the relative LIF signals at 30 and 70 Torr, and applying the necessary quenching correction, a peak NO concentration of $1\text{-}3 \times 10^{12}$ molecules/cm^3 was obtained at 70 Torr (3.2 ppm).

CH--Excitation and observation were performed in the (0,0) band of the A-X system. There was insufficient absorption to calibrate for an absolute CH concentration. However, the profiles taken at 30 and 70 Torr were used to obtain a ratio of the peak CH concentration at these two pressures, showing a decrease in CH concentration at 70 Torr, with the ratio $[CH]_{30\ Torr}/[CH]_{70\ Torr}$ being 1.7.

H Atoms--Hydrogen atoms were excited to the n = 3 level using two photons near 205 nm, with observation of the Balmer-α $n = 3 \rightarrow n = 2$ emission at 656 nm. In addition to LIF, amplified spontaneous emission (ASE) was also observed along the laser axis in both the forward and backward directions.

All intensity profiles were corrected to account for the Boltzmann fraction of the absorbing level at the local temperature. Profiles in the 30 Torr flame are given in Fig. 2 over a wide range of

measurement well into the burnt gases. For OH and NO, the absolute concentrations are given; for CH only a relative profile was obtained. The time decay measurements showed quenching of NO and CH to be invariant with position, so no quenching corrections were performed; the OH profiles were obtained with a prompt gate so they are not influenced by quenching. Also shown is the OH(A) chemiluminescence profile measured with the laser off, a result of the $CH + O_2$ reaction, which creates OH directly in the emitting $A^2\Sigma^+$ state.

At this point, it is useful to qualitatively describe the profiles of the three species in the 30 Torr flame. CH is sharply peaked at about 1.0 cm above the burner surface, similar to that of the chemiluminescence from OH(A), which is a direct product of the $CH + O_2$ reaction. The concentration of NO, OH, and H rise more slowly above the burner, and extend well past the flame front into the burnt gases. NO displays a bisigmoidal rise and this feature is discussed below. Profiles in the 70 and 120 Torr flames are not shown but are qualitatively similar, including a bisigmoidal NO profile at 70 Torr.

FLAME MODEL CALCULATIONS

A computer model of the chemistry of low pressure methane/air flames was assembled to compare predicted concentrations with the experimental profiles, and to gain some insight into the controlling kinetics. A basic mechanism was constructed, with rate constants of our choice[8] based largely on the recommendations of Warnatz[9] for hydrocarbon oxidation and of Miller and Bowman[2] for the prompt NO submechanism. This latter subset was selected according to the authors' flowcharts, and included $deNO_x$ chemistry. A total of 148 reactions involving 38 species were included. Thermodynamic and transport input are from the Sandia databases,[10] with slight modifications for the thermodynamics of the methylenes, formaldehyde, CH_2OH, and NCO.[8] The OH(A) chemiluminescence is calculated according to production from the $CH + O_2$ reaction, and removal by collisional quenching on a time scale short compared to flow velocities or diffusion.

The flame model calculations were carried out using the Sandia flame code,[11] based on one dimensional fluid flow; it includes thermal diffusion, bimolecular and unimolecular kinetics, and sensitivity analysis for individual chemical reactions. Necessary inputs are the measured pressure and gas flow rates at the burner surface, and the measured temperature profile. Calculations were performed well out into the burnt gases, to a height of 10 cm above the burner for the 30 Torr flame. The cross-sectional area of the flame was assumed constant (see below). Predictions of the model are compared to experiment for order, peak position, width and shape of the species profiles, and the absolute concentrations. These comparisons form sensitive tests of our understanding of the flame chemistry.

SPECIES PROFILES

In Fig. 2, the computed concentrations have been matched to the maximum of the experimental values at 30 Torr. In relative position, the CH and OH(A) chemiluminescence reach their peaks at the half maximum point in the rise of ground state OH, i.e., at the flame front in both experiment and model. However, the predicted widths are slightly too small, by roughly a millimeter for CH, and the CH in the model rises a millimeter too late. This disagreement implies some errors in the chemistry controlling CH production and destruction, and thus entertains the expectation that the model will also be in error with respect to predicted NO production. Since the position of the OH rise is well predicted, it appears the overall oxidation chemistry is being modeled reasonably. The OH(A) chemiluminescence calculation appears to decay too rapidly, suggesting gaps in our mechanistic knowledge or a second production reaction.

The shapes of the NO and OH profiles are also adequately computed, although early OH is underpredicted, and the slight apparent decline of NO in the burnt gases is not calculated. The OH profile shows low but significant concentrations at early time (low height) due to diffusion. The rise and steepness of the OH are well predicted, within 1 mm, as is the decline in the burnt gases

via reaction with CO. The leveling off after 2 cm, the presence of NO at low heights, and the bisigmoidality of the profile are well predicted by calculation. The match in absolute position of the NO rise is also good, although diffusion reduces the sharpness of the rise.

ABSOLUTE CONCENTRATIONS

Absolute concentration measurements form another sensitive test. The calculated peak OH concentration at 30 Torr is 50% above the measured value, just at the estimated confidence limit for the absorption measurement. The NO concentration calculated at 1.75 cm for the 30 Torr flame is 3.7 ppm compared to the measured, calibrated value of 4 ppm. This excellent agreement is surprising, given the uncertainty in the main rate constants to which NO is sensitive, in particular the controlling chemistry involving CH (see below).

Our choice of rate constant for the key $CH + N_2 \rightarrow HCN + N$ is based on the direct shock tube measurement of Dean et al.[12] A preliminary transition state theory extrapolation of these values to the lower temperatures of the flame indicates a simple Arrhenius expression is adequate. The value obtained from this rate constant expression is in substantial agreement at 1500 K with the value recommended by Miller and Bowman[2]. An absolute measurement of the CH concentration was not performed in these experiments. The calculation predicts a peak mole fraction of only 2 ppm, very similar to that from another recent modeling study of a 0.1 atm methane/air flame.[13]

Model calculations were also made for the 70 Torr flame with the same stoichiometry and flow rates, using the measured temperature profile as input. The calculated mole fraction of NO formed is the same, in good agreement with the observed ratio of 0.8. The model also predicts a peak mole fraction of CH at 70 Torr of 35% of the 30 Torr value, which agrees excellently with the observed 0.25 ratio. This good agreement, although at present for a very limited set of conditions, offers encouragement for being able to predict pressure effects on prompt NO formation.

We briefly examined a few aspects of the kinetics associated with the profiles of NO, HCN, and NH. The early peak of NO is due to diffusion and its failure to react away at lower temperature. If we analyze all production rates for NO, there are no significant reactive sources in this region. The rise in NO early in the flame front occurs from the $CH + N_2$ reaction, which forms N atoms that are rapidly converted by oxygen to NO. Examination of reaction rates shows that almost all NO is from the prompt mechanism. The other product from the $CH + N_2$ reaction, HCN, also has a wide distribution showing that it has also diffused back to a nonreactive region, and that it takes longer to burn out. The NH distribution, which is the final step in the HCN oxidation process before N and NO production, occurs later in the calculated flame. These last steps are responsible for the final curvature in the profile near 2 cm. The peak NH concentrations are predicted to be in the 10 ppm range, and its LIF profile could be a useful diagnostic for this last portion of the prompt NO mechanism.

Sensitivity analysis indicates the $CH + N_2$ reaction to be the most important step in NO formation. Quantitative measurement and control of CH and its kinetics are clearly indicated as the key to reduction of NO_x emissions which result from prompt NO chemistry.

CONCLUSIONS

Laser-induced fluorescence measurements have been made of the species OH, CH and NO in a low-pressure methane/air flame and compared with predictions from a detailed computer model. Through measurement of several radicals, assessment of the goodness of the model does not rely on a single species comparison, and we can see which part of the model needs further investigation.

The model prediction of both the NO profile and its absolute concentration in this flame are in excellent agreement with experiments. A sensitivity analysis shows that the key reactions

controlling prompt NO are CH + N_2 plus those which control the CH concentration and position. However, the CH concentration profile is not in such good agreement with experiment.

The development of a measure of the predicted temperature sensitivity shows that this parameter, whose profile is taken as input to the model, is extremely important in NO prediction. Uncertainty in the temperature severely limits the ability to calculate or control the amount of prompt NO formed, even with perfect knowledge of kinetics. This could be particularly important for practical burners with nonpremixed flames where there exist a variety of temperature/ concentration conditions.

The model also makes excellent predictions of the relative concentrations of both NO and CH as the pressure is raised from 30 Torr to 70 Torr. This suggests that the pressure dependence of the reaction rates is properly incorporated, and indicates that the model may be suitable for scaling to yet higher pressures. However, confirmation is needed at more than just this pair of pressures.

The success of the model is encouraging although there remain questions, especially concerning the ability to predict CH. Therefore we do not yet know the predictability of this reaction set, and need to make further measurements with different conditions (pressure and stoichiometry). Absolute measurement of the CH concentration would be a particularly useful addition to the results at hand, and a determination of NH would be valuable.

ACKNOWLEDGEMENT

We appreciate the support for this work, furnished by the Southern California Gas Company.

REFERENCES

1. C. P. Fenimore, Thirteenth Symposium (International) on Combustion, The Combustion Institute, Pittsburgh, 1971, p. 373.

2. J. A. Miller and C. T. Bowman, Prog. Energy Comb. Sci. **15**, 287 (1989).

3. K. J. Rensberger, M. J. Dyer, and R. A. Copeland, Appl. Opt. **27**, 3679 (1988).

4. M. J. Dyer, L. D. Pfefferle, and D. R. Crosley, Appl. Opt. **29**, 111 (1990).

5. K. Kohse-Höinghaus, J. B. Jeffries, R. A. Copeland, G. P. Smith, and D. R. Crosley, Twenty-Second Symposium (International) on Combustion, The Combustion Institute, Pittsburgh, 1988, p. 1857.

6. D. E. Heard, J. B. Jeffries, and D. R. Crosley, Chem. Phys. Lett., in press (1991).

7. K. J. Rensberger, J. B. Jeffries, R. A. Copeland, K. Kohse-Höinghaus, M. L. Wise and D. R. Crosley, Appl. Opt. **28**, 3556 (1989).

8. G. P. Smith, Combust. and Flame, in preparation, 1991.

9. J. Warnatz, in Combustion Chemistry, W. G. Gardiner, Ed., (Springer-Verlag, N. Y., 1984).

10. R. J. Kee, F. M. Rupley, and J. A. Miller, Sandia National Laboratory Report SAND87-8215 (1987); R. J. Kee, J. Warnatz, and J. A. Miller, Sandia National Laboratory Report SAND83-8209 (1983).

11. R. J. Kee, J. F. Grcar, M. D. Smooke, and J. A. Miller, Sandia National Laboratory Report SAND85-8240 (1985).

12. A. J. Dean, R. K. Hanson, and C. T. Bowman, Twenty-Third Symposium (International) on Combustion, The Combustion Institute, Pittsburgh, 1991, in press.

13. M. C. Drake and R. J. Blint, Western States Meeting of the Combustion Institute, Paper 90-08, San Diego, Oct. 1990; General Motors Research Publication GMR-6922, 1990.

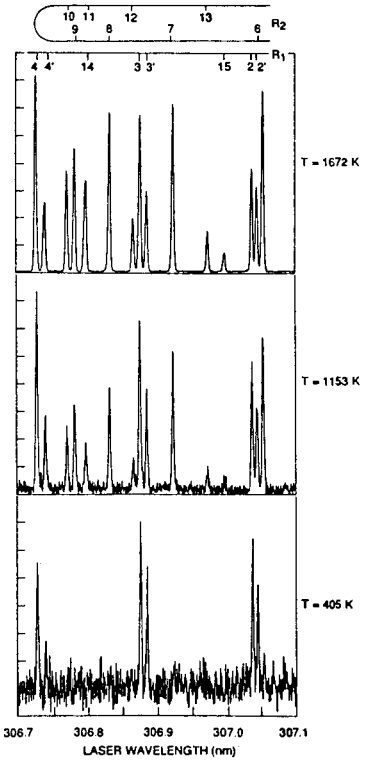

Figure 1 OH LIF rotational excitation spectra at three positions above the burner in the 30 Torr flame. Top: 3.22 cm height, 1672 K temperature; middle: 0.89 cm, 1153 K; bottom: 0.25 cm, 405 K.

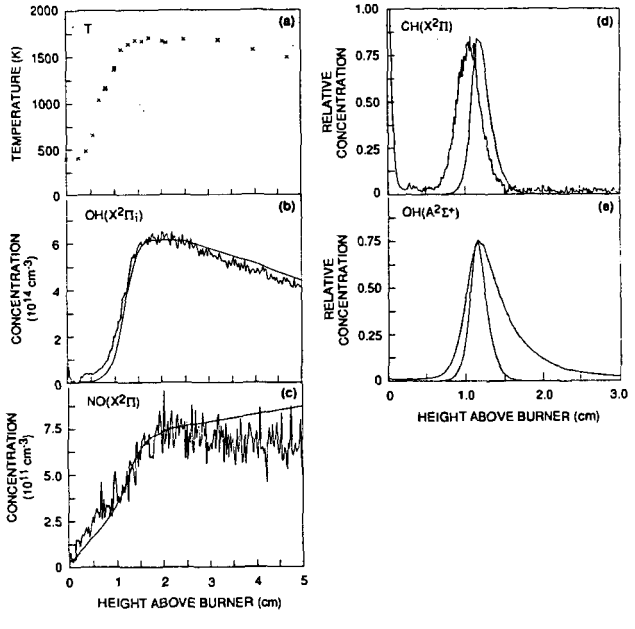

Figure 2 (a) Experimental temperature profile from OH LIF in the 30 Torr flame. A temperature of 399 K at the burner surface was assumed as a boundary condition for the flame model.

(b) - (e) Experimental and calculated species concentration profiles in the 30 Torr $\Phi = 1.13$ methane/air flame. Note the horizontal scale change for (d) $CH(X^2\Pi)$ and (e) $OH(A^2\Sigma^+)$. Model profile species are given by the smooth lines, and the OH values have been scaled by a factor of 0.67 to match the peak experimental value. Scattered laser light from the burner surface can be seen in the CH profile (d).